
This is an electronic reprint of the original article.
This reprint may differ from the original in pagination and typographic detail.

Author(s): Kokkonen, Kimmo & Kaivola, Matti

Title: Scanning heterodyne laser interferometer for phase-sensitive absolute-amplitude measurements of surface vibrations

Year: 2008

Version: Final published version

Please cite the original version:

Kokkonen, Kimmo & Kaivola, Matti. 2008. Scanning heterodyne laser interferometer for phase-sensitive absolute-amplitude measurements of surface vibrations. *Applied Physics Letters*. Volume 92, Issue 6. 063502. ISSN 0003-6951 (printed). DOI: 10.1063/1.2840183.

Rights: © 2008 American Institute of Physics (AIP). This article may be downloaded for personal use only. Any other use requires prior permission of the author and the American Institute of Physics.
<http://scitation.aip.org/content/aip/journal/apl>

All material supplied via Aaltodoc is protected by copyright and other intellectual property rights, and duplication or sale of all or part of any of the repository collections is not permitted, except that material may be duplicated by you for your research use or educational purposes in electronic or print form. You must obtain permission for any other use. Electronic or print copies may not be offered, whether for sale or otherwise to anyone who is not an authorised user.

Scanning heterodyne laser interferometer for phase-sensitive absolute-amplitude measurements of surface vibrations

Kimmo Kokkonen and Matti Kaivola

Citation: [Applied Physics Letters](#) **92**, 063502 (2008); doi: 10.1063/1.2840183

View online: <http://dx.doi.org/10.1063/1.2840183>

View Table of Contents: <http://scitation.aip.org/content/aip/journal/apl/92/6?ver=pdfcov>

Published by the [AIP Publishing](#)

Articles you may be interested in

[Phase sensitive absolute amplitude detection of surface vibrations using homodyne interferometry without active stabilization](#)

J. Appl. Phys. **108**, 114510 (2010); 10.1063/1.3504636

[Damping of surface acoustic vibration induced by electrons trapped on SnO₂ nanocrystal surface](#)

Appl. Phys. Lett. **95**, 211903 (2009); 10.1063/1.3266870

[Optical generation of long-lived surface vibrations in a periodic microstructure](#)

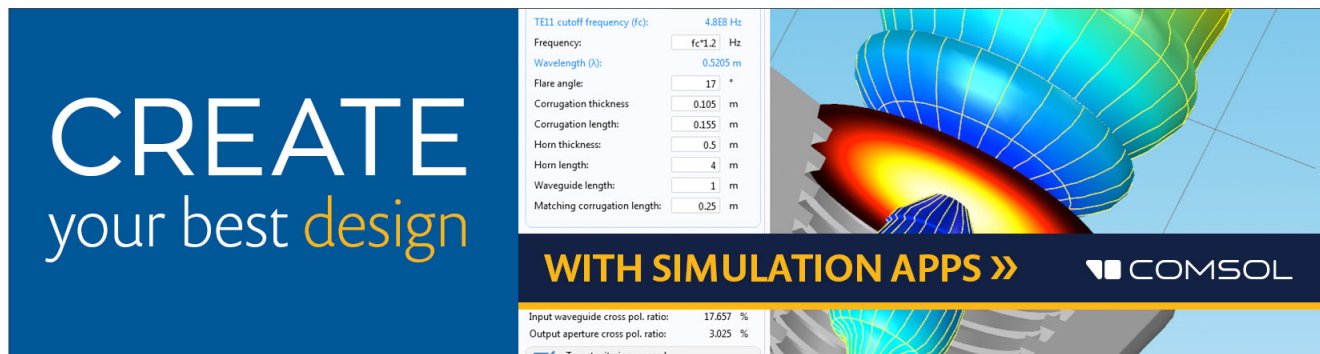
J. Appl. Phys. **105**, 123530 (2009); 10.1063/1.3153956

[Novel phase measurement technique of the heterodyne laser interferometer](#)

Rev. Sci. Instrum. **76**, 093105 (2005); 10.1063/1.2038527

[A multiplexed two-wave mixing interferometer for laser ultrasonic measurements of material anisotropy](#)

AIP Conf. Proc. **615**, 984 (2002); 10.1063/1.1472903

The advertisement features a dark blue background on the left with the text 'CREATE your best design' in white and yellow. On the right, there is a 3D simulation of a horn antenna with a color gradient from blue to red. A white control panel is overlaid on the simulation, listing various parameters and their values. At the bottom right, the COMSOL logo is visible.

TE11 cutoff frequency (fc): 4.868 Hz	
Frequency:	fc*1.2 Hz
Wavelength (λ):	0.5205 m
Flare angle:	17 °
Corrugation thickness:	0.105 m
Corrugation length:	0.155 m
Horn thickness:	0.5 m
Horn length:	4 m
Waveguide length:	1 m
Matching corrugation length:	0.25 m

WITH SIMULATION APPS >> COMSOL

Input waveguide cross pol. ratio:	17.657 %
Output aperture cross pol. ratio:	3.025 %
<input checked="" type="checkbox"/> Target criterion: passed	

Scanning heterodyne laser interferometer for phase-sensitive absolute-amplitude measurements of surface vibrations

Kimmo Kokkonen^{a)} and Matti Kaivola

Optics and Molecular Materials Laboratory, Helsinki University of Technology, P.O. Box 3500, FI-02015 TKK, Finland

(Received 5 December 2007; accepted 15 January 2008; published online 12 February 2008)

We describe a scanning heterodyne interferometer for imaging surface vibrations with a wide frequency range, with current electronics, up to 6 GHz. The heterodyne operation facilitates measurement of absolute amplitude and phase of the surface vibration without calibration. Currently, the setup allows detection of vibration amplitudes down to ~ 1 pm with a lateral resolution of < 1 μm . The interferometer is designed to accommodate the different sample types, e.g., surface and bulk acoustic wave devices and micromechanical resonators. The absolute-amplitude and phase information allows for a thorough characterization of surface vibrations in such components and provides direct information of the vibration fields not obtainable via electrical measurements. © 2008 American Institute of Physics. [DOI: 10.1063/1.2840183]

Recent advances in wireless communication systems have led to extensive research and development of high-frequency, low-loss filters based on surface acoustic wave (SAW) and bulk acoustic wave (BAW) technologies. Furthermore, microelectromechanical system (MEMS) resonators are under intense research, e.g., due to the potential they offer as replacements for conventional reference oscillators, with improved performance and additional benefits of integration into silicon circuits. To develop better components that have their operation based on mechanical vibrations, it is important to be able to directly study the actual vibration fields. Consequently, optical setups based on various techniques¹⁻⁸ have been developed in order to facilitate noncontact vibration measurements that do not disturb the device operation.

Ideally, an optical probe should provide both amplitude and phase information of the studied surface vibration. It should be able to scan both large and small areas with high measurement speed and with a high lateral resolution. Furthermore, the probe should be applicable to measuring modern high-frequency devices. In this letter, we describe the design and operation of a heterodyne interferometer that allows the mapping and analyzing of vibration fields having vibration amplitudes as small as 1 pm, with a lateral resolution better than 1 μm . The heterodyne concept enables acquisition of both absolute amplitude of the surface vibration and its phase, irrespective of variations in the local optical surface reflectance.

The ability to map the amplitude and phase data of a given device opens up a wealth of possibilities for further data analysis. The absolute-amplitude measurements enable, e.g., exact quantitative analysis of SAW attenuation along the propagation direction. The phase information combined with the amplitude data allow powerful data analysis when two-dimensional Fourier methods are applied. For instance, the contributions of standing and propagating waves within a device can be separated, the acoustic reflections analyzed, and dispersion curves extracted. Furthermore, in the case of, e.g., BAW devices, the ability to measure dispersion proper-

ties facilitates extraction of the material parameters of the deposited thin films. In addition, by stepping the phase, the dynamics of the vibration fields can be visualized in order to bring further insight into the device operation.

Consider the interference of two laser beams with intensities I_1 and I_2 originating from the same laser source. If one of the beams is shifted in frequency from the original optical frequency f to $f + f_m$ ($f_m \ll f$), the interference signal averaged over the optical cycle is

$$I(t) = I_1 + I_2 + 2\sqrt{I_1 I_2} \cos[2\pi f_m t + \varphi(t)], \quad (1)$$

where $\varphi(t)$ is the optical phase difference between the beams. When one of the beams is reflected back from a sinusoidally vibrating sample surface, the phase difference can be written as

$$\varphi(t) = \varphi_0 - \frac{4\pi}{\lambda} A \cos(2\pi f_{\text{vib}} t + \phi), \quad (2)$$

where A is the amplitude of the normal component of the surface vibration, λ is the wavelength of the laser light, and f_{vib} and ϕ are the frequency and phase of the vibration, respectively. The term φ_0 is a slowly varying (compared to f_{vib}) phase term that represents any arbitrary optical phase variations between the two arms of the interferometer due to, e.g., variations in the ambient conditions. When the surface-vibration amplitude (A) is small compared to λ , the interference term of Eq. (1) may be expanded as⁹

$$I_{12}(t) = 2\sqrt{I_1 I_2} \left[\cos(2\pi f_m t + \varphi_0) + \frac{2\pi A}{\lambda} \{ \cos[2\pi(f_m + f_{\text{vib}})t + \phi + \varphi_0] - \cos[2\pi(f_m - f_{\text{vib}})t - \phi + \varphi_0] \} \right]. \quad (3)$$

The error in calculated amplitudes due to this approximation is less than 1%, when $A \leq 10$ nm and $\lambda = 632.8$ nm.

When observed in the frequency domain, the signal consists of the modulation peak (f_m) and two satellite peaks ($f_m \pm f_{\text{vib}}$). When measuring actual samples, only the

^{a)}Electronic mail: kimmo.kokkonen@tkk.fi.

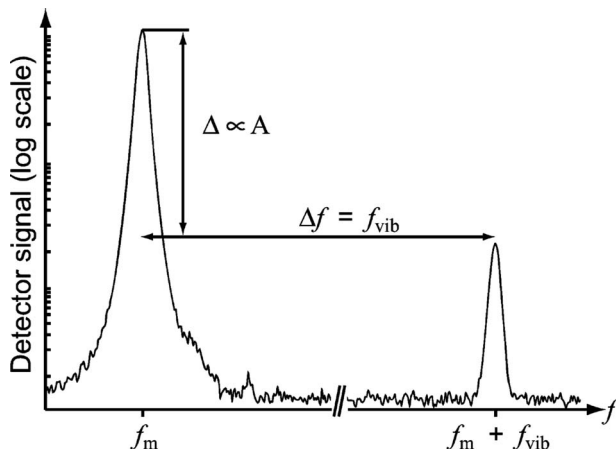


FIG. 1. Typical frequency spectrum of the photodetector signal consisting of a modulation peak at f_m and of a signal peak at $f_m + f_{\text{vib}}$.

modulation peak and the upper ($f_m + f_{\text{vib}}$) satellite peak (hereafter called the signal peak) are detected (see Fig. 1). The modulation and signal peaks (two frequencies) are detected simultaneously, and the absolute amplitude of the surface vibration can be acquired from their amplitude ratio. Also, by comparing the phases of the two peaks, the phase of the surface vibration is acquired, and any slow variations in the optical path lengths cancel out. The ability to measure the absolute amplitude of the surface vibration provides immunity to, e.g., variations in the local optical surface reflectivity of the sample. Furthermore, the heterodyne detection diminishes radio frequency (rf) leakage problems as there is a frequency offset between the detected frequency ($f_m + f_{\text{vib}}$) and the frequency at which the sample is driven (f_{vib}).

The optical layout of the heterodyne interferometer, depicted in Fig. 2, is that of a modified Mach-Zehnder interferometer. A linearly polarized and collimated beam from a single-mode HeNe laser (Spectra-Physics model 117A) is split into two in an acousto-optical modulator (AOM) (IntraAction model AOM-405A1). The frequency-shifted beam (I in Fig. 2) acts as a reference beam while the zeroth-order beam (0) is the probe beam that propagates to the sample and back. The probe beam is focused with a microscope objective (Nikon 50 \times /0.55 ELWD) to an \sim 820 nm sized spot (full width at half maximum) on the sample surface. The $\lambda/4$ plate rotates the polarization plane of the probe beam to facilitate correct beam steering at the polarizing beam splitter (PBS), where the two, now orthogonally polarized, beams are combined. The beams then propagate through a linear polarizer to a fast (0–12 GHz) photodetector (PD), featuring a flat frequency response (better than ± 1 dB up to 6 GHz) (New Focus model 1554-A).

The heterodyne laser interferometer features a sample holder with six degrees of freedom. This allows the sample to be correctly oriented with respect to the probe beam (tilt and rotation) and translation of the sample along three axes. The scanning of the sample is accomplished by computer-controlled linear motor stages (Newport M-MFN25cc) providing a 25 mm range of motion along each axis, with the smallest incremental step size of 55 nm. The interferometer setup is computer controlled and uses point-to-point scanning with a frequency sweep at each spatial point. Using frequency sweep enables fast scan-

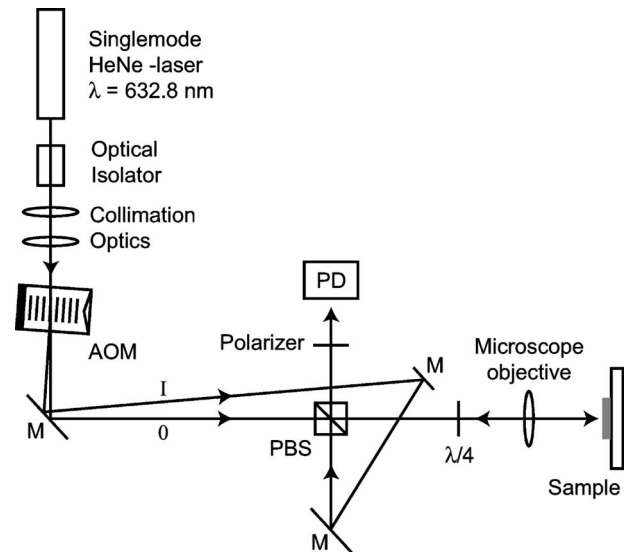


FIG. 2. Optical setup of the heterodyne interferometer: PBS—polarizing beamsplitter, M—mirror, AOM—acousto-optical modulator, and PD—high speed photodetector.

ning, since a single areal scan serves to measure multiple frequencies.

With the current setup and a detection bandwidth of 30 Hz, the smallest detectable surface vibration is ~ 1 pm, as measured with an actual sample. This corresponds to a measurement sensitivity of $\sim 2 \times 10^{-4}$ nm/ $\sqrt{\text{Hz}}$. The theoretical detection limit for a heterodyne interferometer (perfect interference, shot noise limited detection) is given by^{10,11}

$$A_{\min} = \sqrt{\frac{2eB\lambda}{\alpha P_0 \pi}}, \quad (4)$$

where e is the elementary charge, B the detection bandwidth, P_0 the total optical power, α the responsivity (A/W) of the photodetector, and λ the wavelength of the laser. Using the values of 0.5 mW for the optical power, 0.2 A/W for the responsivity, and 632.8 nm for the laser wavelength results in a theoretical detection limit of $\sim 1 \times 10^{-5}$ nm/ $\sqrt{\text{Hz}}$, which with 30 Hz detection bandwidth corresponds to $A_{\min} \sim 0.05$ pm. The difference between the obtained and theoretical sensitivity is mainly due to the limited optical power available at the photodetector, which results in reduction of the available dynamic range. The measurement speed of the system depends on the chosen detection bandwidth. Using the 30 Hz detection bandwidth results in scanning speed of ~ 94 000 points/h, which can be increased by choosing a larger detection bandwidth.

As an example of measurement data, we present selected scanning results from a solidly mounted BAW resonator operating at 932 MHz. The sample geometry and structure along with electrical characteristics are presented in Fig. 3. The sample is fabricated on a glass substrate, which allows for focusing the laser beam through the glass to the bottom of the acoustic mirror stack. The absolute-amplitude detection enables direct comparison of the vibration fields measured, under different optical conditions, from both sides of the sample. Therefore, using absolute-amplitude and phase information, the performance of the acoustical mirror stack can be studied in detail.¹² The measurement is demanding, since the highest vibration amplitudes on top of the resonator

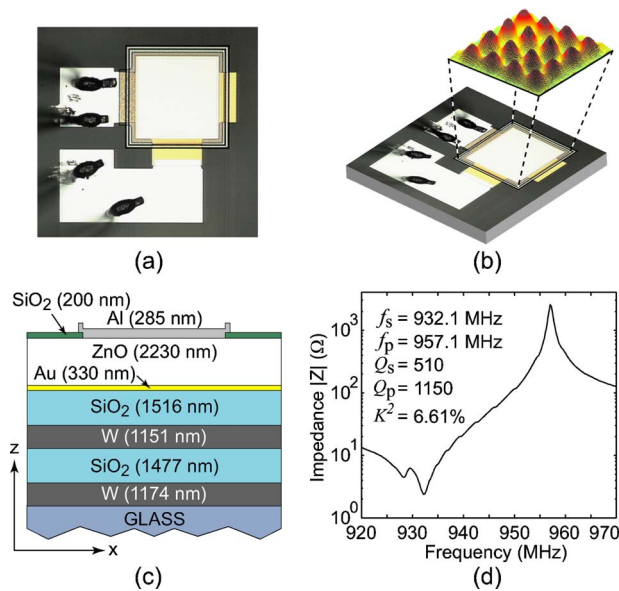


FIG. 3. (Color online) (a) Photograph of a BAW resonator, (b) example of measured amplitude distribution at 938 MHz, (c) schematic representation of the layer stack, and (d) measured impedance response.

are on the order of 300 pm, and the acoustical mirror provides an isolation of ~ 35 dB, resulting in maximum amplitudes of the order of 5 pm on the bottom of the mirror stack. Examples of measured vibration and phase fields on top of the resonator are presented in Figs. 4(a) and 4(b). The corresponding vibration fields at the bottom of the mirror stack are presented in Fig. 4(c) along with Fig. 4(d) corresponding Fourier-filtered amplitude images.

This letter reports a scanning heterodyne laser interferometer for studying high-frequency surface-vibration fields on, e.g., SAW, BAW, and MEMS components. The interferometer setup enables accurate characterization, in terms of both absolute amplitude and phase, of the surface vibration and, hence, is a versatile instrument for research on the physics of the vibrations and for applied research of electroacoustic devices. So far, the setup has been used to characterize SAW, BAW, and MEMS devices, with operating frequencies ranging from 3 MHz to over 2.5 GHz. For recent results on SAW phononic crystals, see Ref. 13. The interferometer provides absolute amplitude, high sensitivity, phase, spatial scanning, high lateral resolution, and high speed. Furthermore, the inertness to rf leakage is essential when measuring modern high-frequency devices.

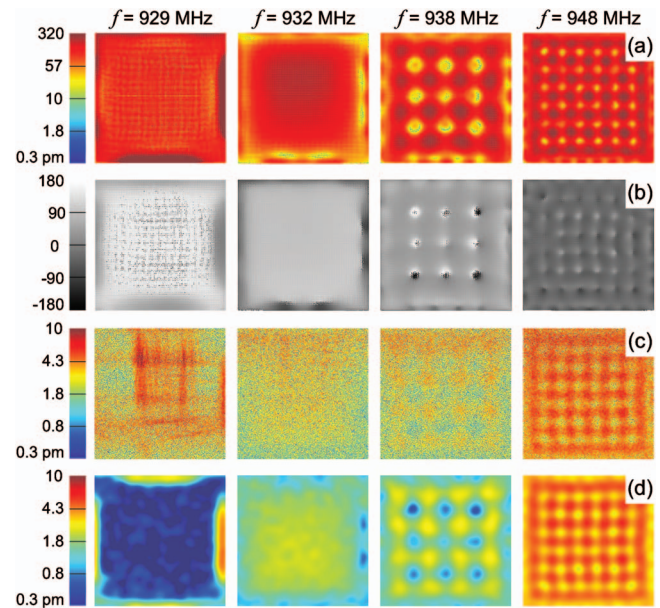


FIG. 4. (Color) (a) Amplitude and (b) phase images of the vibration fields on top of the resonator, and (c) amplitude at the bottom of the acoustic mirror stack. (d) Fourier-filtered amplitude images of (c) with suppressed noise reveal similar vibration fields as on top of the resonator. All the scans cover the active area of the resonator ($297 \times 297 \mu\text{m}^2$) with a lateral step size of $0.99 \mu\text{m}$, resulting in 90 000 data points in each image.

K. Kokkonen thanks Finnish Cultural Foundation and Nokia Foundation for scholarships.

- ¹H. E. Engan, IEEE Trans. Sonics Ultrason. **SU-25**, 372 (1978).
- ²J. V. Knuutila, P. T. Tikka, and M. M. Salomaa, Opt. Lett. **25**, 613 (2000).
- ³J. E. Graebner, B. P. Barber, P. L. Gammel, D. S. Greywall, and S. Gopani, Appl. Phys. Lett. **78**, 159 (2001).
- ⁴S. Rooth, S. Bardal, T. Viken, O. Johansen, and E. Halvorsen, Proc.-IEEE Ultrason. Symp. **1**, 201 (2001).
- ⁵H. Yatsuda, S. Kamiseki, and T. Chiba, Proc.-IEEE Ultrason. Symp. **1**, 13 (2001).
- ⁶G. G. Fattinger and P. T. Tikka, Appl. Phys. Lett. **79**, 290 (2001).
- ⁷K. L. Telschow, V. A. Deason, D. L. Cottle, and J. D. Larson, IEEE Trans. Ultrason. Ferroelectr. Freq. Control **50**, 1279 (2003).
- ⁸H. Martinussen, A. Aksnes, and H. E. Engan, Opt. Express **15**, 11370 (2007).
- ⁹J. P. Monchalin, Rev. Sci. Instrum. **56**, 543 (1985).
- ¹⁰R. L. Whitman and A. Korpel, Appl. Opt. **8**, 1567 (1969).
- ¹¹J. W. Wagner and J. B. Spicer, J. Opt. Soc. Am. B **4**, 1316 (1987).
- ¹²K. Kokkonen and T. Pensala, Proc.-IEEE Ultrason. Symp., 460 (2006).
- ¹³K. Kokkonen, S. Benchabane, A. Khelif, V. Laude, and M. Kaivola, Appl. Phys. Lett. **91**, 083517 (2007).